Check for updates

View Article Online
View Journal

Journal of
Materials Chemistry C

Accepted Manuscript

This article can be cited before page numbers have been issued, to do this please use: H. Guo, J. Yang, B. Pu, H. Chen, Y. Li, Z. M. Wang and X. Niu, *J. Mater. Chem. C*, 2018, DOI: 10.1039/C8TC00683K.

This is an Accepted Manuscript, which has been through the Royal Society of Chemistry peer review process and has been accepted for publication.

Accepted Manuscripts are published online shortly after acceptance, before technical editing, formatting and proof reading. Using this free service, authors can make their results available to the community, in citable form, before we publish the edited article. We will replace this Accepted Manuscript with the edited and formatted Advance Article as soon as it is available.

You can find more information about Accepted Manuscripts in the author guidelines.

Please note that technical editing may introduce minor changes to the text and/or graphics, which may alter content. The journal's standard Terms & Conditions and the ethical guidelines, outlined in our author and reviewer resource centre, still apply. In no event shall the Royal Society of Chemistry be held responsible for any errors or omissions in this Accepted Manuscript or any consequences arising from the use of any information it contains.

ROYAL SOCIETY OF CHEMISTRY

rsc.li/materials-c

View Article Online
DOI: 10.1039/C8TC00683K

Journal of Materials Chemistry C

ARTICLE

Excellent microwave absorption of lead halide perovskites with high stability

Received 00th January 20xx,
Accepted 00th January 20xx

DOI: 10.1039/x0xx00000x

www.rsc.org/

Heng Guo,[a] Jian Yang,[a] Bingxue Pu,[a] Haiyuan Chen,[a] Yulan Li,[a] Zhiming Wang,[b] and Xiaobin Niu*[a,b]

Given the remarkable progress in physical and structural performances of organic-inorganic lead halide perovskites as a superstar in the photovoltaic field, the study of some of their intrinsic properties are still missing. Herein, we report the microwave absorption performance in $MAPbX_3$ (MA = $CH_3NH_3^+$, X = I^-, Br^- or Cl^-) perovskite crystals in terms of complex permittivity and permeability. We find that the $MAPbI_3$, $MAPbBr_3$ and $MAPbCl_3$ perovskites possess excellent microwave absorbability, and the optimum reflect losses reach -55.23, -54.70 and -46.44 dB at 16.77, 15.46 and 13.54 GHz with a matching thickness of 1.62, 1.76 and 1.95 mm, respectively. Thereafter, we explore the absorption mechanism and find that the microwave absorption properties are ascribed to the combination of dielectric loss and magnetic loss, but mainly for dielectric loss. In addition, the stability of microwave absorbability is also investigated and it is proved to be significantly depend on the decomposition of corresponding perovskites. These results highlight the importance to the discovery of microwave absorbability in organic-inorganic lead halide perovskites. More importantly, our study provides perovskite absorbers as a new variable to be considered in the quest for future microwave devices.

Introduction

Organic-inorganic lead halide perovskites have attracted significant attentions as promising semiconductors since their potentials have been successfully implemented in lasers,[1-2] photodetectors,[3-5] X-ray detectors,[6-7] light-emitting diodes,[8-10] hydrogen production,[11-12] and high-efficiency solar cells,[13-15] etc. Particularly, $MAPbX_3$ (MA = $CH_3NH_3^+$, X = I^-, Br^- or Cl^-) perovskites can combine facile and low-cost solution fabrication techniques with their favorable intrinsic properties such as tunable direct optical band gap,[16] high-absorption coefficients,[17] long carrier lifetime,[18] and high carrier mobility[19]. Similar to other traditional semiconductors, these unique physical properties provide a view of the ultimate potential of $MAPbX_3$ perovskites, and make high-quality $MAPbX_3$ perovskite single crystals much broader in optoelectronic applications than their thin polycrystalline film counterparts.[20-21] Currently, some detailed fundamental and intrinsic properties of organic-inorganic perovskite crystals are still under debate. Despite the stunning developments in perovskite semiconductors performance, the microwave absorbing properties of $MAPbX_3$ perovskites have not yet been studied.

Microwave absorption materials can absorb microwave energy and reduce electromagnetic backscatter effectively, by converting electronic microwave energy into electric, thermal and magnetic energy or dissipating electromagnetic wave by interference,[22-23] have become increasingly important in electronic equipment, not only for communication systems, but also for military affairs, such as mobile phone, wireless local area network, satellite broadcast systems, and so on.[24] Generally, microwave absorption characteristics of a material, which combine dielectric properties and magnetic properties, depend on their intrinsic electromagnetic properties (i.e. electronic conductivity, complex permittivity and permeability) as well as extrinsic properties such as thickness and working frequency. The traditional microwave absorbers such as ferrite, metallic particles, carbon-based materials, and ceramics are still in use these days.[25-26] Moreover, microwave absorber composites containing dielectric, magnetic, or hybrid components, including organic-functionalized inorganic $BaTiO_3$ perovskites, have attracted extensive interests because of their high permeability, high electric resistivity and high resonance frequency.[27-28] Although the microwave absorbing mechanism of those materials is believed mainly based on either dielectric loss or magnetic loss, these claims still lack the conclusive support of related and available evidence to interpret microwave absorption properties of organic-inorganic perovskite semiconductor materials.

Here we directly probed the microwave absorbing properties of $MAPbI_3$, $MAPbBr_3$ and $MAPbCl_3$ perovskite crystals using conventional transmission/reflection technique. Specifically, the simulated reflection loss values for $MAPbI_3$, $MAPbBr_3$ and $MAPbCl_3$ perovskites are -55.23, -54.70 and -46.44 dB, respectively, indicating excellent microwave absorbability in the microwave range. Moreover, long-term stability of the microwave absorption properties of $MAPbX_3$ perovskite crystals is also demonstrated. These findings further emphasize the versatility and performance potential of inorganic-organic lead halide perovskite materials for the development of perovskite-based microwave devices.

[a] State Key Laboratory of Electronic Thin Film and Integrated Devices, School of Materials and Energy, University of Electronic Science and Technology of China, Chengdu 610054, P. R. China. *Email: xbniu@uestc.edu.cn
[b] Institute of Fundamental and Frontier Sciences, University of Electronic Science and Technology of China, Chengdu 610054, P. R. China.
Electronic Supplementary Information (ESI) available. See DOI: 10.1039/x0xx00000x

Published on 17 March 2018. Downloaded by Fudan University on 17/03/2018 05:47:22.

Journal of Materials Chemistry C Accepted Manuscript

Please do not adjust margins

View Article Online
DOI: 10.1039/C8TC00683K

Published on 17 March 2018. Downloaded by Fudan University on 17/03/2018 05:47:22.

Journal of Materials Chemistry C Accepted Manuscript

Experimental

Materials

Lead iodide (PbI_2, 99 %), lead bromide ($PbBr_2$, 99 %), lead chloride ($PbCl_2$, 99 %) were purchased from Aladdin. Methylamine (CH_3NH_2, 33 wt.% in absolute ethanol), hydroiodic acid (HI, 57 wt.% in water), hydrobromic acid (HBr, 48 wt.% in water) and hydrochloric acid (HCl, 37 wt.% in water) were also obtained by Aladdin. Solvents including anhydrous *N*, *N*-dimethylformamide (DMF, 99.8%), anhydrous dimethyl sulfoxide (DMSO, 99.8%), gamma-butyrolactone (GBL, anhydrous, 99%) were supplied by Sigma-Aldrich. All the chemicals were used directly without any further purification.

Synthesis of methylammonium halide (MAX)

Methylammonium halides (MAX, MA) = $CH_3NH_3^+$, X = I, Br, Cl) were synthesized according to the previous report with modifications.[34] Typically, 34 mL methylamine and 38 mL HX (X = I, Br, Cl) solution were mixed in a 150 mL three-necked flask at 0 °C for 2 h in an ice-water bath. After that, the solvent was removed by rotary evaporating at 50 °C for 1 h, the resulting white product was washed with diethyl ether and then recrystallized from ethanol, repeated three times, and finally dried at 60 °C overnight in a vacuum oven. In the end, snow-white MAI, MABr, MACl crystals were obtained.

Grown of $MAPbX_3$ perovskite single crystals

$MAPbX_3$ (X = I, Br or Cl) single crystals were grown using a facile evaporative crystallization growth (ECG) method with modifications.[29] The equimolar mixture of the prepared MAX and PbX_2 (X = I, Br or Cl) were dissolved under vigorous stirring in GBL, DMF and DMSO at 60 °C, respectively. The corresponding solution concentration was controlled at 1.2 M, 1.0 M and 2.0 M, respectively. As-prepared perovskite precursor solutions were heated and kept on a 100 °C hotplate overnight. Black, orange and colorless small crystals appeared as the heating time increases. To make the crystal larger, small seed crystals were placed into the corresponding flesh perovskite precursor solutions at 100 °C, and kept for 12 ~ 24 h until larger crystals were grown. Subsequently, by using the larger crystals as new seeds and repeating the above process, the crystals with even larger size were obtained. Finally, bulk $MAPbI_3$, $MAPbBr_3$ and $MAPbCl_3$ single crystals were hot DMF to get rid of the leftover solution form the surface and dried in a vacuum oven at 80 °C for 6 h.

Structural characterizations

The as-prepared perovskite singles crystals and corresponding powders were characterized by X-ray diffraction (XRD, Rigaku RINT2400, Japan) with Cu Kα (λ = 0.1541 nm) radiation at 45 kV and 40 mA. Thermal gravimetric analysis (TGA) was performed on a TA Instruments Q50. The samples (10-15 mg) were heated from ambient to 500 °C at a heating rate of 20 °C·min^{-1} under nitrogen flow with a purge of 40 ml min^{-1}. The optical images of $MAPbI_3$ and $MAPbBr_3$ seed crystals were obtained on an Olympus BX51M optical microscope. The Ultraviolet-Visible (UV-vis) absorption spectra were recorded with TU-1810PC spectrophotometer in the wavelength range of 300-800 nm in transmission mode.

Microwave absorption characterizations

For measuring microwave absorption, these samples were prepared with perovskite crystal powders loading in paraffin. The bulk $MAPbX_3$ single crystals samples were pulverized and mixed with paraffin in a mass ratio of 3 : 1, and then pressed into a cylindrically shaped compact with an inner diameter of 3.0 mm and an outer diameter of 7.0 mm (Length: 5.0 mm). Next, the cylindric samples were tightly sandwiched by two measured fixtures with the coaxial inner and outer conductors attaching two electrodes. Then, the real (ε′ and μ′) and imaginary (ε″ and μ″) parts of the relative complex permittivity and permeability of these samples were investigated using a vector network analyzer (Agilent 8720ET) in the frequency range of 0.5-18 GHz. Finally, we carried out microwave absorption properties measurements with the transmission/reflection method, in which the reflection loss (RL) were calculated using the relative complex permittivity ε_r ($\varepsilon_r = \varepsilon' - j\varepsilon''$) and permeability μ_r ($\mu_r = \mu' - j\mu''$) at a given frequency and thickness layer.

Results and discussion

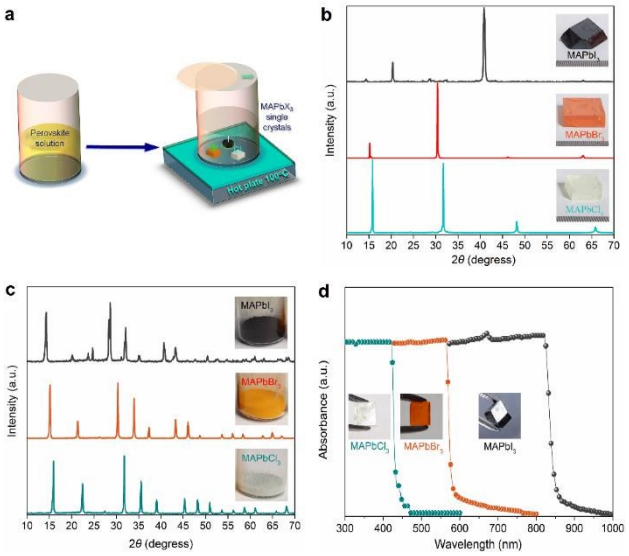

Fig. 1 a) A schematic illustration of $MAPbX_3$ (X = I, Br or Cl) single crystal preparation. XRD patterns of $MAPbX_3$ b) single crystals and c) powders. The inset images show photographs of b) bulk large $MAPbX_3$ single crystals (crystal size ~ 10 mm) and c) $MAPbX_3$ crystal powders. d) Visible absorbance spectrum of $MAPbX_3$ single crystals and the inset images show photographs of small bulk $MAPbX_3$ single crystals (crystal size ~ 5 mm).

We synthesized high-quality bulk $MAPbX_3$ (X = I, Br or Cl) single crystals using a facile evaporative crystallization growth (ECG) technique proposed by Liu and colleagues[29], with modifications. As depicted in Fig. 1a, we prepared perovskite precursor solutions by mixing methylammonium halides (MAX, X = I, Br or Cl) with corresponding lead halides (PbX_2, X = I, Br or Cl) and solvents (GBL for I, DMF for Br, DMSO for Cl, respectively) to form an unsaturated solution on a 100 °C hotplate. Subsequently, the seal cap of evaporation dish that control the evaporation rate of solvent played an important role in the rate of single crystal growth. With the evaporation of solvent, seed crystals (see Fig. S1a and S1b) appeared when the solution was saturated or supersaturated. Next, seed crystallites were added into flesh perovskite precursor solutions at 100

This journal is © The Royal Society of Chemistry 20xx

Please do not adjust margins

View Article Online
DOI: 10.1039/C8TC00683K

Published on 17 March 2018. Downloaded by Fudan University on 17/03/2018 05:47:22.

Journal of Materials Chemistry C Accepted Manuscript

°C, and maintained for 12 ~ 24 h until larger crystals was grown. By using larger crystals as new seeds and repeating the above process, the crystals (Seen in Fig. S1c and S1d) with appropriate sizes were obtained. X-ray diffraction (XRD) patterns of $MAPbX_3$ (X = I, Br or Cl) single crystals demonstrate the pure perovskite phase for $MAPbI_3$, $MAPbBr_3$, $MAPbCl_3$ (Fig. 1b), confirming high quality of single crystals[2,30-31]. The inset images show photographs of the $MAPbI_3$, $MAPbBr_3$, $MAPbCl_3$ single crystals with dimensions of ~14×13×2.2, ~11×11×2.0 and ~7×7×2.0 mm^3. Meanwhile, the XRD characterizations of $MAPbX_3$ powders crushed from corresponding single crystals were also performed in Fig. 1c. The corresponding patterns show a set of strong diffraction peaks that can be assigned to pure tetragonal $MAPbI_3$[32], cubic $MAPbBr_3$[33] and cubic $MAPbCl_3$[3] crystal structures. Moreover, the visible absorbance spectrum of bulk $MAPbX_3$ single crystals were investigated. As shown in Fig. 1d, it is clear that the light is absorbed strongly for bulk $MAPbX_3$ single crystals with the absorption onsets at ~ 860 nm, ~ 600 nm and ~ 450 nm, respectively, which is in good matching with the absorbance of three typical $MAPbX_3$ perovskite crystals.[20,29,34] The analyses on the absorption spectra of single crystals gave their optical bandgaps of 1.45, 2.15 and 2.83 eV, respectively (Fig. S2a). In addition, the thermal stability of bulk $MAPbX_3$ single crystals were investigated in Fig. S2b-S2d, which is similar to the decomposition behaviour of classic high quality $MAPbX_3$ perovskite single crystals.[29]

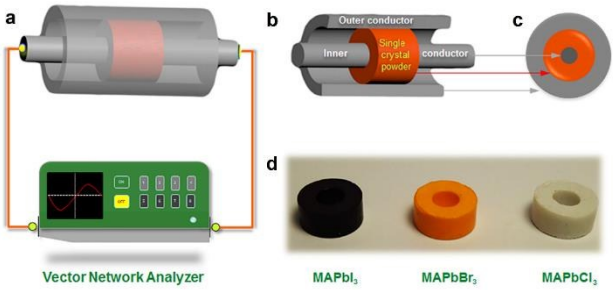

Fig. 2 a) Schematic drawing of the experimental set-up for microwave absorption measurement for $MAPbX_3$ (X = I, Br or Cl) crystal samples. Schematics of the b) cross-section and c) top view of the measured sample. d) Photographs of the measured $MAPbX_3$ crystal samples.

Fig. 2a schematically depicts the experimental set-up for the microwave characteristic measurements. The transmission/reflection method [35] was carried out by using a vector network analyzer in the frequency range of 0.5-18 GHz. The device can show reflected and transmitted transient responses when an incident wave pulse is radiated by a free space transmission path to the toroidal samples (Fig. S3). The sample was tightly sandwiched by two electrodes with the coaxial inner and outer conductors, and schematics of the cross-section and top view of the measured specimen fixture are shown in Fig. 2b and 2c. The powder crystal circular rings were fabricated by mixing $MAPbX_3$ crystals and paraffin as illustrated in Fig. 2d (See the experimental section). Here, we simulated the reflection loss (RL) of the as-prepared $MAPbX_3$ (X = I, Br or Cl) samples using the transmit line theory of electromagnetism absorption, which was demonstrated to be an effective model for a single-layer plane-wave absorber. In this model, the RL value can be calculated from the measured relative complex permittivity and complex permeability data for the given absorber thickness and microwave frequency using the following equation:[36]

$$RL\ (dB) = 20 \log |\Gamma| = 20 \log |(Z_{in}-Z_0)/(Z_{in}+Z_0)| \quad (1)$$

Where Γ is the reflection coefficient, Z_{in} is the input characteristic impedance of the absorber, which can be obtained from the following expression:

$$Z_{in} = Z_0\sqrt{(\mu_r/\varepsilon_r)}\tanh[j(2\pi fd/c)\sqrt{\mu_r\varepsilon_r}] \quad (2)$$

Where f is the frequency of the microwave in free space, c is the velocity of light in vacuum, and d is the thickness of the absorber. ε_r ($\varepsilon_r = \varepsilon' - j\varepsilon''$) and μ_r ($\mu_r = \mu' - j\mu''$) are the measured relative complex permittivity and permeability, respectively. Z_0 is the intrinsic impedance of free space and given by the formula:

$$Z_0 = \sqrt{\mu_0/\varepsilon_0} = 376.7\ \Omega \quad (3)$$

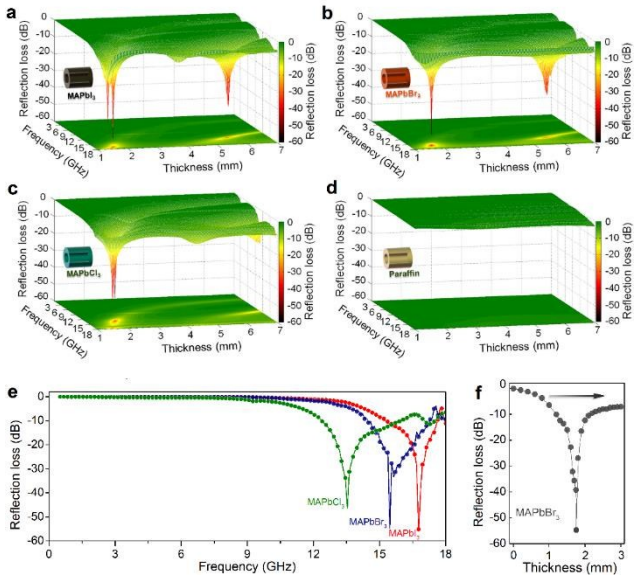

Fig. 3 3D color plots of numerical simulated reflection loss versus thickness as a function of frequency: a) $MAPbI_3$, b) $MAPbBr_3$, c) $MAPbCl_3$ and d) paraffin samples. e) Microwave absorption curves of the best performed $MAPbX_3$ crystal samples with optimal thicknesses. f) Microwave absorption curves of $MAPbBr_3$ crystal samples versus thickness.

Table 1 The optimal microwave absorption parameters of these measured samples.

Samples	Frequency (GHz)	Thickness (mm)	Reflection loss (dB)
$MAPbI_3$	16.77	1.62	-55.23
$MAPbBr_3$	15.46	1.76	-54.70
$MAPbCl_3$	13.54	1.95	-46.44
PbI_2	18.00	2.03	-4.58
$PbBr_2$	18.00	1.82	-6.87
$PbCl_2$	18.00	1.69	-12.73
MAI	15.99	2.60	-3.13
MABr	18.00	2.24	-3.00
MACl	18.00	2.34	-2.762
Paraffin	16.6	3.54	-2.945

Please do not adjust margins

View Article Online
DOI: 10.1039/C8TC00683K

Published on 17 March 2018. Downloaded by Fudan University on 17/03/2018 05:47:22.

The 3D presentations of the calculated theoretical RL data of the $MAPbX_3$ (X = I, Br or Cl) samples with varying frequencies and thicknesses are exhibited in Fig. 3a-3c. Compared with the pure paraffin wax sample (Fig. 3d), all the $MAPbX_3$ samples exhibit excellent microwave absorptions in two thickness ranges of 1.0-2.5 mm and 4.0-7.0 mm at high frequency of 12-18 GHz (Ku-band frequency). The optimal microwave absorbing parameters are summarized in Table 1. On the basis of the optimal thickness in the classical range of 1-5 mm, the minimum RL peak values of the $MAPbI_3$, $MAPbBr_3$ and $MAPbCl_3$ samples are -55.23, -54.70 and -46.44 dB at 16.77, 15.46 and 13.46 GHz with a thickness of 1.62, 1.76 and 1.95 mm, respectively (Fig. 3e). It is clearly seen that the optimal peak intensity gradually increase from Cl to Br and I, and the peaks move to the high frequency region with the decreasing thickness. Additionally, the optimization of thickness for the $MAPbBr_3$ sample is also demonstrated in Fig. 3f. There is one narrow and strong microwave absorbing peak as the thickness increases. Obviously, the thickness of the sample is one of the crucial parameters that affect the intensity and location of the frequency with RL minimum.[37] On the basis of these results, it can be found that all the organic-inorganic $MAPbX_3$ crystal samples exhibit excellent microwave absorption properties with appropriate thickness at high frequency.

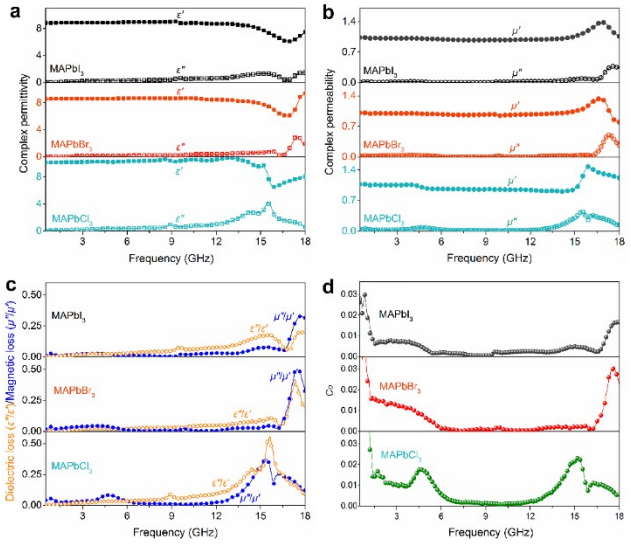

Fig. 4 a) Complex permittivity (ε' and ε"), b) complex permeability (μ' and μ"), c) dielectric loss/magnetic loss and d) C_o ($C_o = \mu''(\mu')^{-2}f^{-1}$) curves of $MAPbX_3$ (X = I, Br or Cl) crystal samples.

To evaluate the microwave absorption performance of the perovskite samples, the lead salts (PbI_2, $PbBr_2$ and $PbCl_2$) and organic halides (MAI, MABr and MACl) as the raw material of the perovskites display very low RL values at low thickness (See in Table 1). It is interesting that both $PbBr_2$ and $PbCl_2$ samples show excellent microwave absorption only with large thickness (> 5.0 mm) at high-frequency regime (Fig. S4 and Table S1, Supporting Information), which is useful to improve microwave absorptivity of $MAPbX_3$ perovskites with large thickness. However, it is the fact that PbI_2 sample shows relative low microwave absorption in the whole thickness range. Moreover, the MAI, MABr and MACl powder samples exhibit hardly any microwave absorption at the whole range of frequency. Thereby, there might be a possible reason that the special structural characteristics result in the electromagnetic wave absorptions of the organic-inorganic $MAPbX_3$ perovskite crystals.

In order to investigate the microwave absorption mechanism of the perovskite samples, we independently measured the complex relative permittivity and permeability of $MAPbX_3$ crystal samples. Fig. 4a shows the frequency dependence of the real (ε') and imaginary (ε") parts of the relative complex permittivity ($\varepsilon_r = \varepsilon' - j\varepsilon''$) of $MAPbX_3$ (X = I, Br or Cl) crystal samples. It can be seen that the ε' values of the three $MAPbI_3$, $MAPbBr_3$ and $MAPbCl_3$ crystal samples decrease with the increase of frequency and exhibit their minimum values of 6.1, 6.0 and 6.5 with respect to the frequency of 16.9, 16.7 and 15.9 GHz, respectively. It is concluded that the distinct dielectric response characteristic is demonstrated as dielectric dispersion.[38-39] Moreover, the $MAPbI_3$, $MAPbBr_3$ and $MAPbCl_3$ crystal samples demonstrate relatively low ε″ values with the maxima of 1.4, 2.8 and 4.4 at 17.8, 17.3 and 15.5 GHz, respectively, suggesting the occurrence of strong resonance. For comparison, the ε″ values of PbX_2 and MAX (X = I, Br and Cl) samples maintain almost constant 0 (see Fig. S5 and S6). According to the free-electron theory,[40] the ε″ value can be summarized as the following equation:

$$\varepsilon'' = \frac{\sigma}{2\varepsilon_0 \pi f} \quad (4)$$

Where σ represents electric conductivity, f is the frequency of the microwave in free space, and ε_0 is the permittivity of free space ($\varepsilon_0 = 8.854 \times 10^{-12}$ F m^{-1}). It is confirm that the low ε″ means low conductivity and causes low electric polarization. This is because organic-inorganic lead halide perovskite is a typical semiconductor material with direct bandgap. However, it is well known that $MAPbX_3$ perovskites have very high carrier mobility,[41] which may result in electron polarization with strong dielectric loss. Furthermore, the plotting of ε″ versus ε′ is shown in Fig. 5. As for $MAPbX_3$ samples, one or two Cole-Cole semicircles are clearly observed and distorted, which is consistent with Debye dipolar relaxation model and indicate the occurrence of dielectric relaxation process.[42] This also suggests that the permittivity at microwave frequency can be contributed by dipole relaxation polarization.[39,43-44]

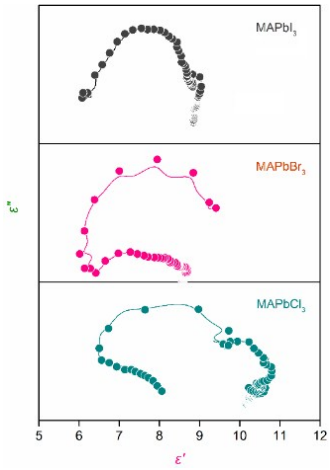

Fig. 5 The real part (ε') versus imaginary (ε") plots of complex permittivity of $MAPbX_3$ (X = I, Br or Cl) crystal samples.

Journal of Materials Chemistry C Accepted Manuscript

This journal is © The Royal Society of Chemistry 20xx

Please do not adjust margins

View Article Online
DOI: 10.1039/C8TC00683K

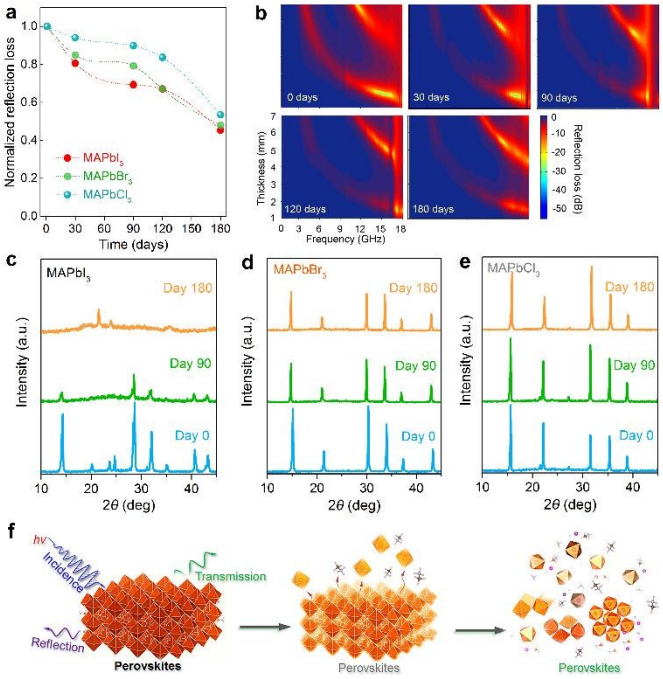

Fig. 6 a) The long-term stability of microwave absorption properties of $MAPbX_3$ (X = I, Br or Cl) crystal samples. b) 2D color plots of numerical simulated reflection loss of $MAPbBr_3$ crystal samples versus thickness and frequency as a function of time. XRD patterns of c) $MAPbI_3$, d) $MAPbBr_3$ and e) $MAPbCl_3$ crystal samples were measured as function time stored in N_2. f) The proposed microwave absorbing degradation mechanism of the $MAPbX_3$ crystal samples.

The real (μ') and imaginary (μ") parts of the relative complex permeability μ_r ($\mu_r = \mu' - j\mu''$) versus frequency for $MAPbX_3$ (X = I, Br or Cl) crystal samples are shown in Fig. 4b, which represent the storage and loss capability of magnetic energy, respectively. Obviously, the μ' and μ" of $MAPbX_3$ samples almost maintained constant (1 and 0, respectively), exhibiting no magnetic loss in the 0.5-12 GHz frequency range. However, the μ' of $MAPbI_3$, $MAPbBr_3$ and $MAPbCl_3$ crystal samples demonstrates a slight increase and the values of μ' are 1.4, 1.3 and 1.5 at frequency 16.9, 16.6 and 15.9 GHz, respectively. Similarly, the corresponding μ" values are 0.4, 0.5 and 0.3 with corresponding frequency at 17.7, 17.3 and 15.6 GHz, respectively. It suggests that magnetic loss still happens despite of the absence of non-magnetic properties in these perovskites. After that, we calculated the dielectric loss ($\tan\delta_\varepsilon = \varepsilon''/\varepsilon'$) and magnetic loss ($\tan\delta_\mu = \mu''/\mu'$) as dissipation factors (Fig. 4c). As illustrated in Fig. 4c, the $\tan\delta_\varepsilon$ of all the $MAPbX_3$ samples exhibit two resonance peaks around 14-18 GHz, indicating the perovskites exhibit intense dielectric losses. It is further confirmed that the loss mechanisms are attributed to dominant dipolar polarization and associated relaxation phenomena.[25] Meanwhile, the tan δ_μ also demonstrates similar characteristics with that of the μ'', implying that the loss mechanism of the perovskites includes magnetic loss. Generally, the microwave magnetic loss of magnetic materials mainly results from magnetic hysteresis, domain-wall displacement, natural resonance and eddy current loss.[45] It is well known that the C_0 value can be summarized as the following equation:

$$C_0 = \mu''(\mu')^{-2}f^{-1} = \frac{2\pi\mu_0\sigma d^2}{3} \quad (5)$$

Where μ_0 is the permeability of free space and σ represents electric conductivity. If the magnetic loss from eddy-current loss, the C_0 values should be constants when the frequency varies. However, the values of C_0 have two strong resonance peaks as a function of frequency (Fig. 4d). Thus, it can be concluded that the magnetic loss for $MAPbX_3$ perovskites is mainly ascribed to the natural resonance, which makes the behaviors of dielectric and magnetic losses more complex.

In spite of the excellent microwave absorption capabilities, one major concern is the poor stability as for organic-inorganic lead halide perovskites, which is a barrier to practical applications. We therefore monitored the long-term stability in microwave absorption of these perovskite samples. The $MAPbX_3$ crystal samples were tested without encapsulation and exposed directly to the environment at 25 °C with 30-50 % humidity. Fig. 6a presents the optimal RL values of the $MAPbX_3$ crystal samples as a function of storage time in nitrogen atmosphere. In terms of the RL data of the perovskite samples, the microwave absorptivity remains 80 % up to 30 days, while the RL values are degraded to almost 50 % after 180 days. Such exceptional stability can be attributed to the robustness introduced by paraffin, which forms compact and stable circular rings, again as a consequence of the inhomogeneous degradation of different perovskite/paraffin composites. In particular, as for $MAPbBr_3$ crystal samples, the degradation of microwave absorption versus frequency and thickness, is displayed in Fig. 6 b. Notably, the microwave absorption ability gradually decreases as the storage time increases in small thickness ranges of 1.0-2.5 mm, while increases as the storage time increases in large thickness ranges of 4.0-7.0 mm. It is clearly revealed that the degradation of the microwave absorption is likely due to decomposition of the $MAPbBr_3$ perovskite along with the increasing of $PbBr_2$ component. To obtain more in-depth understanding of the mechanism behind the observed degradation in the microwave absorption, XRD measurements of the surface of $MAPbX_3$ crystal samples (Photographs in Fig. S7) were carried out in Fig. 6c-6e. As depicted in Fig. 6c, it is clear the $MAPbI_3$ perovskite-related peaks at scattering angles 2θ = 14.3° (110), 28.6 ° (220) and 43.2 ° (330) have disappeared after stored in N_2 for 180 days. However, the intensity of the peaks of $MAPbBr_3$ and $MAPbCl_3$ samples show a small reduction (Fig. 6d and 6e), strongly suggesting the less degradation of the perovskites. Interestingly, for three perovskite samples, there is no peak at 12.5°, corresponding to the absence of PbI_2. The finding points to no transformation from $MAPbX_3$ to PbX_2 without loss of MAX, again suggests that the encapsulation of the paraffin on the perovskite is of the utmost importance to protect the decomposition of the perovskites. From our results, there may be another reason that the electromagnetic waves can be effectively absorbed by the perovskites and converted into thermal energy, which caused by the intrinsic instability of the organic-inorganic perovskites (Fig. 6f).

Conclusions

In summary, for the first time, we have investigated the microwave absorption performance of $MAPbI_3$, $MAPbBr_3$, and $MAPbCl_3$ perovskite crystal powders using the transmit line

Published on 17 March 2018. Downloaded by Fudan University on 17/03/2018 05:47:22.

Journal of Materials Chemistry C Accepted Manuscript

Please do not adjust margins

theory of electromagnetism absorption. With the simulation of reflection loss, we have discovered the extremely excellent microwave absorbability in these perovskites. More importantly, the mechanism of the microwave absorption properties has been discussed in detail. The final verdict is that the outstanding microwave absorption properties are ascribed to the electromagnetic match in perovskite structure, the lags of polarization and strong natural resonance. Finally, we also note that the long-term stability of microwave absorbability significantly dependents on the decomposition of corresponding perovskites. Our results show the perovskite absorbers as a new variable to be consider in the quest for future microwave devices.

Conflicts of interest

There are no conflicts to declare.

Acknowledgements

The authors acknowledge the financial support from the Recruitment Program of Global Young Experts of China and Sichuan one thousand Talents Plan.

Notes and references

1 G. Xing, N. Mathews, S. S. Lim, N. Yantara, X. Liu, D. Sabba, M. Gratzel, S. Mhaisalkar, T. C. Sum, *Nat. Mater.,* 2014, **13**, 476-480.

2 H. Zhu, Y. Fu, F. Meng, X. Wu, Z. Gong, Q. Ding, M. V. Gustafsson, M. T. Trinh, S. Jin, X. Y. Zhu, *Nat. Mater.,* 2015, **14**, 636-642.

3 V. Adinolfi, O. Ouellette, M. I. Saidaminov, G. Walters, A. L. Abdelhady, O. M. Bakr, E. H. Sargent, *Adv. Mater.,* 2016, **28**, 7264-7268.

4 M. I. Saidaminov, V. Adinolfi, R. Comin, A. L. Abdelhady, W. Peng, I. Dursun, M. Yuan, S. Hoogland, E. H. Sargent, O. M. Bakr, *Nat. Commun.,* 2015, **6**, 8724.

5 Y. Fang, Q. Dong, Y. Shao, Y. Yuan, J. Huang, *Nat. Photonics,* 2015, **9**, 679-686.

6 S. Yakunin, M. Sytnyk, D. Kriegner, S. Shrestha, M. Richter, G. J. Matt, H. Azimi, C. J. Brabec, J. Stangl, M. V. Kovalenko, W. Heiss, *Nat. Photonics,* 2015, **9**, 444-449.

7 H. Wei, Y. Fang, P. Mulligan, W. Chuirazzi, H.-H. Fang, C. Wang, B. R. Ecker, Y. Gao, M. A. Loi, L. Cao, J. Huang, *Nat. Photonics,* 2016, **10**, 333-339.

8 Z. K. Tan, R. S. Moghaddam, M. L. Lai, P. Docampo, R. Higler, F. Deschler, M. Price, A. Sadhanala, L. M. Pazos, D. Credgington, F. Hanusch, T. Bein, H. J. Snaith, R. H. Friend, *Nat. Nanotechnol.,* 2014, **9**, 687-692.

9 A. Swarnkar, A. R. Marshall, E. M. Sanehira, B. D. Chernomordik, D. T. Moore, J. A. Christians, T. Chakrabarti, J. M. Luther, *Science,* 2016, **354**, 92-95.

10 H. Cho, S. H. Jeong, M. H. Park, Y. H. Kim, C. Wolf, C. L. Lee, J. H. Heo, A. Sadhanala, N. Myoung, S. Yoo, S. H. Im, R. H. Friend, T. W. Lee, *Science,* 2015, **350**, 1222.

11 J. Luo, J. H. Im, M. T. Mayer, M. Schreier, M. K. Nazeeruddin, N. G. Park, S. D. Tilley, H. J. Fan, M. Gratzel, *Science,* 2014, **345**, 1593-1596.

12 M. Crespo-Quesada, L. M. Pazos-Outón, J. Warnan, M. F. Kuehnel, R. H. Friend, E. Reisner, *Nat. Commun.,* 2016, **7**, 12555.

13 S. S. Shin, E. J. Yeom, W. S. Yang, S. Hur, M. G. Kim, J. Im, J. W. Seo, J. H. Noh, S. Seok, S*cience,* 2017, **356**, 167.

14 H. Tan, A. Jain, O. Voznyy, X. Z. Lan, F. P. G. Arquer, J. Z. Fan, R. Quintero-Bermudez, M. J. Yuan, B. Zhang, Y. C. Zhao, F. J. Fan, P. C. Li, L. N. Quan, Y. B. Zhao, Z. H. Lu, Z. Y. Yang, S. Hoogland, E. H. Sargent, *Science,* 2017, **355**, 722-726.

15 J. N. Chen, S. S. Zhou, S. Y. Jin, H. Q. Li and T. Y. Zha, *J. Mater. Chem. C.*, 2016, **4**, 11-27.

16 D. P. McMeekin, G. Sadoughi, W. Rehman, G. E. Eperon, M. Saliba, M. T. Hörantner, A. Haghighirad, N. Sakai, L. Korte, B. Rech, M. B. Johnston, L. M. Herz, H. J. Snaith, *Science,* 2016, **351**, 151-155.

17 H. S. Kim, C. R. Lee, J. H. Im, K. B. Lee, T. Moehl, A. Marchioro, S. J. Moon, R. Humphry-Baker, J. H. Yum, J. E. Moser, M. Gratzel, N. G. Park, *Sci. Rep.,* 2012, **2**, 591.

18 C. Wehrenfennig, G. E. Eperon, M. B. Johnston, H. J. Snaith, L. M. Herz, *Adv. Mater.,* 2014, **26**, 1584-1589.

19 G. Xing, N. Mathews, S. Sun, S. S. Lim, Y. M. Lam, M. Gratzel, S. Mhaisalkar, T. C. Sum, *Science,* 2013, **342**, 344-347.

20 M. I. Saidaminov, A. L. Abdelhady, B. Murali, E. Alarousu, V. M. Burlakov, W. Peng, I. Dursun, L. Wang, Y. He, G. Maculan, A. Goriely, T. Wu, O. F. Mohammed, O. M. Bakr, *Nat. Commun.,* 2015, **6**, 7586.

21 H. H. Fang, S. Adjokatse, H. T. Wei, J. Yang, G. R. Blake, J. S. Huang, J. Even, M. A. Loi, *Sci. Adv.,* 2016, **2**, 7.

22 P. B. Liu, Y. Huang, X. Zhang, *Compos. Sci. Technol.,* 2014, **95**, 107-113.

23 F. Qin, C. Brosseau, *J. Appl. Phys.,* 2012, **6**, 061301-061301-24.

24 V. K. Singh, A. Shukla, M. K. Patra, L. Saini, R. K. Jani, S. R. Vadera, N. Kumar, *Carbon,* 2012, **50**, 2202-2208.

25 J. Liu, R. Che, H. Chen, F. Zhang, F. Xia, Q. Wu, M. Wang, *Small,* 2012, **8**, 1214-1221.

26 C. Song, X. Yin, M. Han, X. Li, Z. Hou, L. Zhang, L. Cheng, *Carbon,* 2017, **116**, 50-58.

27 B. W. Li, Y. Shen, Z. X. Yue, C. W. Nan, *Appl. Phys. Lett.,* 2006, **89**, 132504.

28 R. C. Che, L. M. Peng, X. F. Duan, Q. Chen, X. L. Liang, *Adv. Mater.,* 2004, **16**, 401-405.

29 Y. Liu, Z. Yang, D. Cui, X. Ren, J. Sun, X. Liu, J. Zhang, Q. Wei, H. Fan, F. Yu, X. Zhang, C. Zhao, S. F. Liu, *Adv. Mater.,* 2015, **27**, 5176-5183.

30 Y. Zhou, L. You, S. Wang, Z. Ku, H. Fan, D. Schmidt, A. Rusydi, L. Chang, L. Wang, P. Ren, L. Chen, G. Yuan, L. Chen, J. Wang, *Nat. Commun.,* 2016, **7**, 11193.

31 Y. Yang, Y. Yan, M. Yang, S. Choi, K. Zhu, J. M. Luther, M. C. Beard, *Nat. Commun.,* 2015, **6**, 7961.

32 M. I. Saidaminov, M. A. Haque, M. Savoie, A. L. Abdelhady, N. Cho, I. Dursun, U. Buttner, E. Alarousu, T. Wu, O. M. Bakr, *Adv. Mater.,* 2016, **28**, 8144-8149.

33 Y. X. Chen, Q. Q. Ge, Y. Shi, J. Liu, D. J. Xue, J. Y. Ma, J. Ding, H. J. Yan, J. S. Hu, L. J. Wan, *J. Am. Chem. Soc.* 2016, *138*, 16196-16199.

34 L. Dimesso, M. Dimamay, M. Hamburger, W. Jaegermann, *Chem. Mater.,* 2014, **26**, 6762-6770.

View Article Online
DOI: 10.1039/C8TC00683K

Published on 17 March 2018. Downloaded by Fudan University on 17/03/2018 05:47:22.

Journal of Materials Chemistry C Accepted Manuscript

This journal is © The Royal Society of Chemistry 20xx

Please do not adjust margins

View Article Online
DOI: 10.1039/C8TC00683K

35 A. M. Nicolson, G. F. Ross, IEEE Trans. Instrum. Meas., 1970, **4**, 377-382.
36 Y. F. Pan, G. S. Wang, L. Liu, L. Guo, S. H. Yu, *Nano Research,* 2016, **10**, 284-294.
37 G. Sun, B. Dong, M. Cao, B. Wei, C. Hu, *Chem. Mater.,* 2011, **23**, 1587-1593.
38 S. Zhao, Z. Gao, C. Chen, G. Wang, B. Zhang, Y. Chen, J. Zhang, X. Li, Y. Qin, *Carbon,* 2016, **98**, 196-203.
39 Y. Duan, Z. Liu, H. Jing, Y. Zhang, S. Li, *J. Mater. Chem.,* 2012, **22**, 18291.
40 H. Yu, T. Wang, B. Wen, M. Lu, Z. Xu, C. Zhu, Y. Chen, X. Xue, C. Sun, M. Cao, *J. Mater. Chem.,* 2012, **22**, 21679.
41 A. Mei, X. Li, L. F. Liu, Z. L. Ku, T. F. Liu, Y. G. Rong, M. Xu, M. Hu, J. Z. Chen, Y. Yang, M. Grätzel, H. W. Han, *Science,* 2014, **345**, 295-298.
42 H. Guo, Y. Zhan, Z. Chen, F. Meng, J. Wei, X. Liu, *J. Mater. Chem. A,* 2013, **1**, 2286-2296.
43 E. Strelcov, Q. F. Dong, T. Li, J. Chae, Y. C. Shao, Y. h. Deng, A. Gruverman, J. S. Huang, A. Centrone, *Sci. Adv.,* 2017, **3**, e1602165.
44 S. Meloni, T. Moehl, W. Tress, M. Franckevicius, M. Saliba, Y. H. Lee, P. Gao, M. K. Nazeeruddin, S. M. Zakeeruddin, U. Rothlisberger, M. Graetzel, *Nat. Commun.,* 2016, **7**, 10334.
45 J. Zhan, Y. Yao, C. Zhang, C. Li, *J. Alloy. Compd.,* 2014, **585**, 240-244.

Published on 17 March 2018. Downloaded by Fudan University on 17/03/2018 05:47:22.

Journal of Materials Chemistry C Accepted Manuscript

Please do not adjust margins

View Article Online
DOI: 10.1039/C8TC00683K

Graphical Abstracts:

Organic-inorganic $CH_3NH_3PbI_3$, $CH_3NH_3PbBr_3$ and $CH_3NH_3PbCl_3$ perovskites possess outstanding microwave absorbability with high reflect loss values.

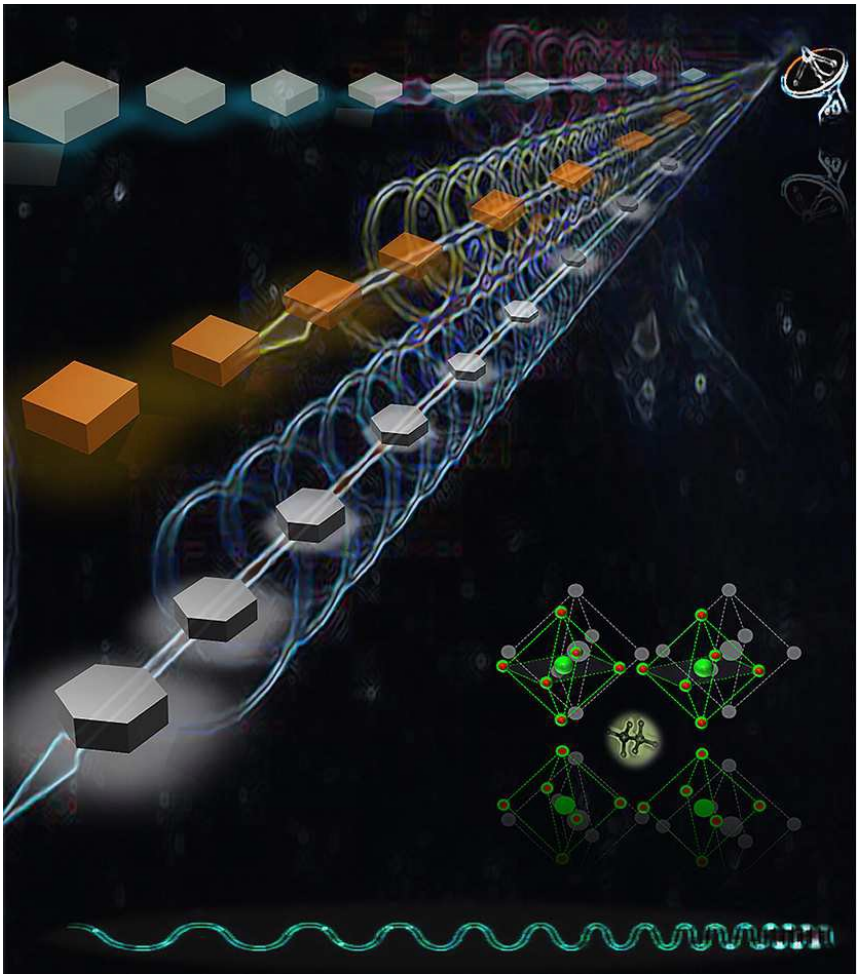

Published on 17 March 2018. Downloaded by Fudan University on 17/03/2018 05:47:22.

Journal of Materials Chemistry C Accepted Manuscript